Research on Distance Measurement System Based on Swept-Source Interferometry

Ruiping Wang*, Jiajia Dong, Xiaomei He, Lei He
Changcheng Institute of Metrology and Measurement (CIMM), Beijing, China
**Corresponding Author*

Abstract: This paper presents the design and implementation of an absolute distance measurement system grounded in the principles of swept-frequency interferometry. The system utilizes a swept-frequency light source with a central wavelength of 1310 nm and a scanning range of 100 nm, integrated with a Mach-Zehnder fiber interferometer and a balanced photodetector to facilitate high-speed acquisition and processing of interference signals. Spectral calibration is achieved via a k-clock-assisted interferometer, enabling preprocessing of the raw signals through equal wavenumber resampling, DC component removal, and Hanning window shaping, effectively suppressing noise and enhancing signal fidelity. Subsequent Fourier transform transposes the interference data from the wavenumber domain to the depth domain, from which peak extraction is performed to resolve absolute distance measurements.

Keywords: Swept-Frequency Interferometry; Distance Measurement; Spectral Calibration; Fourier Transform

1. Introduction

Optical interferometric measurement techniques, owing to their inherent advantages of non-contact operation and high precision, have become indispensable technological pillars in advanced domains such as precision metrology, industrial inspection, and biomedical imaging. Amidst the ongoing transformation of modern manufacturing towards micro- and nano-scale transformation and intelligent automation, the demands placed on absolute distance measurement-encompassing accuracy, speed, and dynamic range-have grown increasingly stringent. These demands necessitate overcoming the inherent limitations of traditional contact-based measurement methods while simultaneously balancing efficient acquisition with superior precision.

Although conventional laser interferometry can achieve ultra-high precision, it is constrained by phase ambiguity effects which induce measurement uncertainties over long-range absolute distance detection, coupled with a limited dynamic measurement range, thereby falling short of the requirements imposed by complex practical scenarios. Low-coherence interferometry, leveraging broadband light sources to attain zero optical path difference localization, fundamentally addresses phase ambiguity and naturally supports absolute distance measurement. However, its reliance on mechanical scanning mechanisms drastically restricts measurement speed, rendering it unsuitable for real-time applications such as high-speed online inspection [1].

Swept-frequency interferometry emerges as an innovative solution that bridges the shortcomings of these preceding techniques. By ingeniously combining the absolute measurement capability of low-coherence interferometry with the rapid imaging strengths of Fourier-domain signal processing [2,3], this technique employs a wavelength-swept source that varies periodically over time. Through the acquisition of interference spectral signals dependent on wavelength, distance information can be directly extracted via Fourier transform without the need for elaborate mechanical scanning apparatus, thereby markedly enhancing measurement efficiency while preserving accuracy. To date, swept-frequency interferometry has been extensively adopted in optical coherence tomography, demonstrating exceptional resolution and imaging speed particularly in biological tissue tomography, thus providing critical technological support for clinical diagnostics.

Against this technical backdrop, this paper endeavors to design and construct a fiber-optic swept-frequency interferometry system tailored for high-precision, non-contact absolute distance measurement in industrial environments. By optimizing the optical architecture and integrating core algorithms including spectral calibration, signal filtering, and Fourier transform, the system achieves accurate absolute distance demodulation. With its compact structure, robust interference immunity, and rapid measurement capabilities, the proposed system adeptly addresses diverse applications such as industrial inspection and precision instrument calibration. It offers a novel technical solution for overcoming the challenges inherent in high-precision distance measurement under complex operational conditions, bearing significant engineering merit and promising potential for widespread deployment.

2. Principle of Swept-Frequency Interferometric Measurement

Swept-frequency interferometric distance measurement technology is fundamentally rooted in the theories of low-coherence interferometry and Fourier transform principles. Its paramount advantage lies in eschewing the dependence on mechanical scanning mechanisms, instead achieving high-speed absolute distance measurement through dynamic, periodic wavelength sweeping of the light source. The system's measurement performance is intrinsically tied to the bandwidth, scanning linearity, and coherence properties of the swept-frequency light source. In this system, a swept-frequency laser source emits light whose wavelength varies linearly and periodically over time. The beam is divided by the interferometer into a reference and a sample arm. When the two beams satisfy the coherence condition-specifically, when their optical path difference is less than the coherence length of the source-they interfere, generating an interference spectral signal that varies with wavelength [4,5]. The frequency characteristics of this interference signal bear a stringent one-to-one correspondence with the measured distance; namely, the greater the distance, the higher the frequency of the interference signal. This intrinsic physical property forms the cornerstone for quantitative distance retrieval.

The intensity of the interference spectral signal can be expressed as:

$$I(k) = P_r + P_0 \int_{-\infty}^{+\infty} h^2(z)\,dz + 2\sqrt{P_r P_O} \int_{-\infty}^{+\infty} h(z)\Gamma(z)\cos\big(2k(t)z + \phi(z)\big)dz \quad (1)$$

Where, Pr denotes the reference optical power detected by the photodetector, Po represents the sample arm power incident on the object, and k(t)=2π/λ(t) is the wavenumber at instant t (with λ(t) being the source wavelength at time t). Γ(z) is the coherence function of the swept-frequency source, and z signifies the depth position. The first two terms correspond to the DC component and autocorrelation terms, respectively-both being interference artifacts that adversely impact the imaging performance of the swept-frequency interferometry system and thus must be minimized. The third term embodies the valuable interferometric information, wherein the amplitude is positively correlated with the coupling efficiency of the reference and sample optical powers, while the phase directly reflects the optical path difference between the two beams. Because this optical path difference linearly relates to the measured distance, performing a Fourier transform on this term:

$$F(z) = \mathcal{F}\{I(k)\} \quad (2)$$

transforms the signal from the wavenumber domain (k-space) into the depth domain (z-space). The location of spectral peaks corresponds to the measured distance. By extracting the positional differences of multiple interface peaks, absolute distance measurement can be accurately realized.

In practical scenarios, the swept-frequency light source exhibits nonlinearity, resulting in non-uniform sampling of the interference signal in the wavenumber domain. Such nonlinearity broadens the spectral peaks after Fourier transform and induces peak shifts, thereby causing measurement errors that notably accumulate in long-range distance measurements. To mitigate this, spectral calibration is indispensable, whereby the signal is resampled at uniformly spaced wavenumber intervals to preserve resolution and measurement accuracy post-Fourier transform. Additionally, environmental variations such as temperature fluctuations and fiber refractive index changes introduce extraneous optical path differences. Hence, the principle-level assurance of system measurement accuracy requires not only algorithmic enhancements but also an optical architecture designed to suppress external disturbances, ensuring that detected optical path changes arise solely from the target's distance variation.

3. Architecture of the Swept-Frequency Interferometric Distance Measurement System

As illustrated in Figure 1, the swept-frequency interferometric distance measurement system designed and implemented herein is anchored around the Mach-Zehnder interferometer (MZI) principle. Through a modular architecture, it achieves seamless integration and high-efficiency coordination among the light source emission, optical path transmission, signal detection, and data acquisition subsystems. The entire system boasts a compact form factor coupled with robust anti-interference capability, thereby fulfilling the rigorous demands of high-precision absolute distance measurement in engineering applications. The core components of the system comprise the swept-frequency light source module, fiber optic interferometer module, signal detection module, and data acquisition and processing module. Each module's parameter selection and structural design are meticulously optimized to balance measurement accuracy, speed, and system stability. Figure 2 depicts the physical realization of the measurement system.

The system employs a swept-frequency light source centered at 1310 nm with a tuning range of 100 nm, providing an ample spectral bandwidth crucial for precise distance resolution. Operating at a sweep frequency of 100 kHz, it markedly enhances measurement efficiency compared to conventional low-coherence interferometry methods reliant on mechanical scanning, thus accommodating rapid detection in dynamic scenarios. The fiber interferometer module, constituting the heart of the optical layout, is implemented as an all-fiber configuration utilizing circulators and couplers to construct the MZI framework. The reference arm is further refined with fiber delay lines to enable flexible adjustment over different measurement ranges. A balanced photodetector with a bandwidth of 1.6 GHz and detection wavelength spanning 1200–1700 nm converts the interferometric optical signal into an electrical counterpart. Leveraging differential detection effectively suppresses common-mode noise, thereby improving signal integrity. The electrical signals are captured by a high-speed data acquisition card operating at 500 MS/s with a 12-bit resolution, which faithfully records the intricate features of the high-frequency interference signals while preventing distortion. High-throughput data transfer between the acquisition card and the computer is facilitated via a PCIe interface, ensuring real-time capture and storage at a 100 kHz scanning rate. Subsequent demodulation is performed by signal processing algorithms executed on the computer. All optical connections employ FC/APC low-loss fiber connectors featuring insertion losses below 0.3 dB, substantially minimizing optical attenuation and thereby safeguarding the stability and reliability of the measurement system.

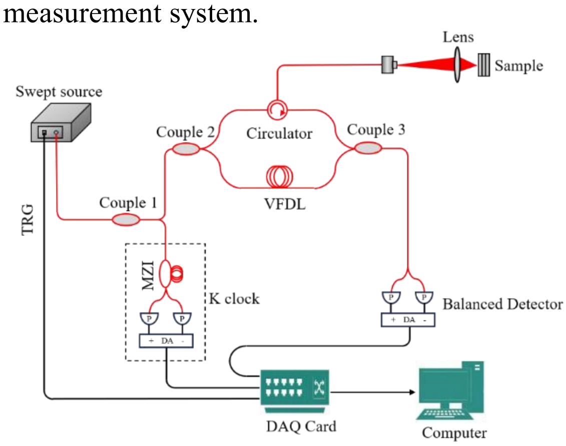

Figure 1. Schematic Diagram of the Swept-Frequency Interferometric Distance Measurement System

Figure 2. Photograph of the Physical Swept-Frequency Interferometric Distance Measurement System

The system's input light emanates from the swept-frequency light source and is initially divided into two beams by Coupler 1. The majority of the optical power is directed into the main Mach-Zehnder interferometric (MZI) sensing path for imaging, while a smaller fraction is routed to the auxiliary interferometer within the k-clock module for spectral calibration purposes. Within the MZI sensing arm, the incident light is further split by Coupler 2 into two parts: one portion serves as the sample beam entering the sample arm, transmitted via Circulator 2 to the system's probe head. The sample-reflected light carrying depth-resolved information is routed back through the circulator to Coupler 3. The other portion constitutes the reference beam, which traverses a fiber delay line before reaching Coupler 3. The fiber delay line is employed to finely adjust the optical path length of the reference arm, ensuring that the optical path difference between the reference and sample arms satisfies the coherence condition for interference at varying sample depths. Coupler 3 recombines the reflected signals from both arms, producing an interference signal imbued with tomographic information of the sample. This interference signal is evenly split into two paths and delivered to a balanced photodetector. The amplified differential output from the balanced photodetector is acquired by the data acquisition card and transmitted to the computer for subsequent processing of the raw data. Through these procedures, the system achieves absolute measurement of the target distance.

4. Interference Signal Demodulation

4.1 Signal Preprocessing

Spectral Calibration: Given that the swept-frequency light source's output wavelength varies periodically and linearly with time, but the laser's wavenumber changes non-uniformly, uniform time-domain sampling of the interference signal results in an uneven distribution of samples in wavenumber (k) space [6,7]. Since the sample depth coordinate z and wavenumber k form a Fourier transform pair, spectral calibration is indispensable. As depicted in Figure 1, a MZI auxiliary interferometer is integrated into the optical path to generate a sinusoidal calibration signal-known as the k-clock. By applying a nearest-neighbor interpolation algorithm, the original interference signal is resampled to achieve equidistant sampling in k-space, effectively eliminating errors induced by nonlinear wavelength variation. The interference signal sampled at equal intervals in k-space is illustrated in Figure 3(a).

DC Component Removal: Although the system utilizes a balanced photodetector to suppress common-mode noise, in practical application the input signals to the two photodetector terminals are not perfectly balanced; consequently, the DC components are not entirely eliminated. Further processing is therefore necessary to mitigate the adverse impact of these residual DC and autocorrelation terms on image quality. This is achieved by averaging one frame of the original two-dimensional cross-sectional data to estimate the system's background noise, then subtracting this noise from every data point. In particular, averaging a set of axial scans and subtracting this mean from each axial scan efficiently removes the DC and autocorrelation components inherent in the interference data.

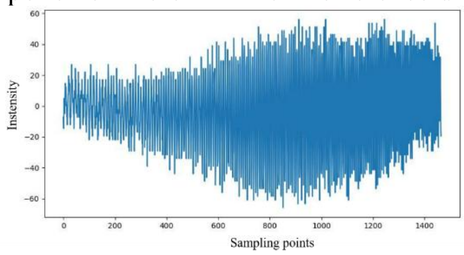

(a) Raw Sampled Data

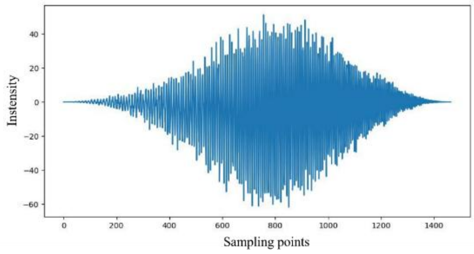

(b) Post-Preprocessing Data

Figure 3. Comparison of Interference Signals before and after Preprocessing

Spectral Shaping: The shape of the interference spectrum envelope significantly influences imaging resolution. The swept-frequency source employed does not exhibit a Gaussian spectral distribution, leading to diminished system resolution and pronounced sidelobes. These sidelobes introduce considerable noise into the imaging results and degrade image contrast. Hence, before performing Fourier transform, the raw interference spectral signal undergoes windowing to refine its envelope. A Hanning window is applied to the DC-removed signal to attenuate sidelobe interference, thereby enhancing the peak discernibility after Fourier transform. The Hanning window function is expressed as:

$$W(k_n)=\frac{1}{2k}\left(1+\cos\frac{\pi k_n}{k}\right) \quad (3)$$

Where, k represents the wavenumber range. Denoting the pre-shaped spectrum as *S(k)*, the shaped spectrum is:

$$S^{'}(k)=W(k)\times S(k) \quad (4)$$

Figure 3(b) depicts the interference signal after

DC component removal and spectral shaping.

4.2 Fourier Transform and Distance Extraction

As illustrated in Figure 4, the preprocessed interference signal undergoes a discrete Fourier transform (DFT) [8-10], converting the data from the wavenumber (k) domain into the spatial depth (z) domain. The interference signal is fundamentally a real-valued function, and thus its Fourier transform exhibits conjugate symmetry. This symmetry manifests in the depth domain as two mirror-image peaks relative to the zero optical path difference. In practical imaging scenarios, as shown in Figure 5, only the positive peak corresponding to the true sample depth is retained, while the negative peak is discarded. By analyzing the magnitude spectrum of the transformed signal, the position of the peak amplitude precisely indicates the measured distance.

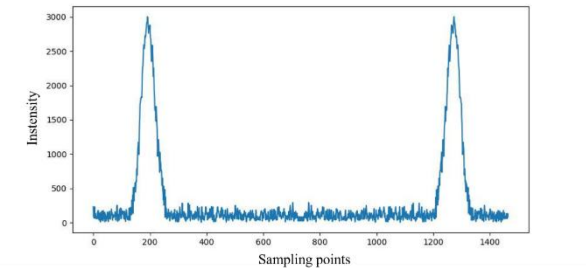

Figure 4. Discrete Fourier Transform

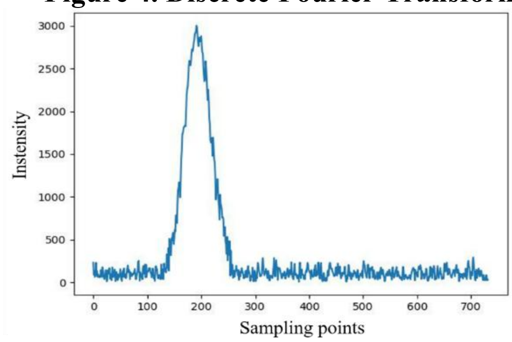

Figure 5. Retention of the Positive Peak in the Fourier Transform

5. Distance Measurement

Using the swept-frequency interferometric distance measurement system constructed herein, a mirror mounted on a high-precision translation stage served as the test specimen, positioned within the measurement depth range. The mirror's axial position along the optical path was precisely measured. By translating the stage to displace the mirror by 1 mm along the beam direction, the returning interference signals were captured and demodulated. The results, illustrated in Figure 6, reveal that the extracted peak position, converted into depth information, corresponds to a displacement of 1.001 mm-matching the actual movement of the mirror.

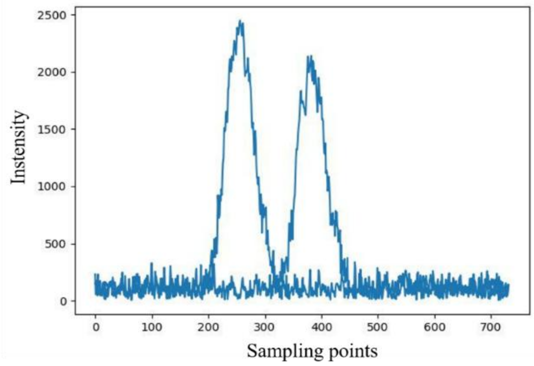

Figure 6. Discrete Fourier Transform of the Interference Signal in Distance Measurement

6. Conclusion

This paper has presented the design and implementation of an absolute distance measurement system founded on swept-frequency interferometry. By integrating a swept-frequency light source with a fiber optic interferometer, the system realizes high-precision, non-contact absolute distance measurement. Boasting a streamlined configuration and robust anti-interference capabilities, the system holds promising potential for further enhancement through the incorporation of scanning galvanometers, rotary probes, and other mechanisms to enable comprehensive measurement of surface geometries and internal cavities. Such advancements would substantially augment the system's performance and versatility, underpinning its considerable prospects for practical engineering applications

References

[1] Ruiping Wang, Xiaomei He, Jiajia Dong, et al. A Study on Distance Measurement System Based on Low-Coherence Interferometry. Journal of Engineering System, 2024, 2(4):46-51.

[2] Gordon S. Kino, Stanley S. C. Chim. Mirau correlation microscope. Applied optics, 1990, 29(26): 3775-3783.

[3] Huang D, Swanson E A, Lin C P, et al. Optical coherence tomography. Science, 1991, 254(5035): 1178-1181.

[4] Chen X, Liu M, Zhang Q, et al. Fiber-Optic Swept-Source Interferometer for Dynamic

Distance Monitoring in Industrial Environments. Optics and Lasers in Engineering, 2022, 156: 107123.
[5] Garcia R, Martinez A, Mendez R, et al. Compact Swept-Source Interferometer System for Biomedical Distance Sensing. Sensors, 2022, 22(19): 7345.
[6] Hu Zw, He B, Xue P, et al. High-speed k-linear swept laser using acousto-optic deflectors with Doppler shift compensation for optical coherence tomography, Optics Letters, 2024, 49(1):101-104.
[7] Zhang Y, Li J, Wang H, et al. High-Precision Absolute Distance Measurement Based on Swept-Source Interferometry with Improved k-Linearization. IEEE Transactions on Instrumentation and Measurement, 2023, 72: 1-9.
[8] Famin Wang, Yongyi Tan, Jingyi Gu, et al. Vibration Measurement Technology of Optical Fiber SS-Oct Based on All-Phase Fast Fourier Transform. Instrumentation, 2025, 12(3): 63-72.
[9] Huang S W, Aguirre A D, Huber R A, et al. Swept source optical coherence microscopy using a Fourier domain mode-locked laser. Optics Express, 2007, 15(10): 6210-6217.
[10] Kim S, Park J, Lee H. Fast Distance Demodulation Algorithm for Swept-Source Interferometry Based on FFT and Peak Extraction Optimization. Measurement Science and Technology, 2023, 34(8): 085006.